

## Far tail ( $255 R_E$ ) fast response to very weak magnetic activity

J.-A. Sauvaud,<sup>1</sup> A. Opitz,<sup>1</sup> L. Palin,<sup>1</sup> B. Lavraud,<sup>1</sup> C. Jacquy,<sup>1</sup> L. Kistler,<sup>2</sup> H. U. Frey,<sup>3</sup>  
J. Luhmann,<sup>3</sup> D. Larson,<sup>3</sup> and C. T. Russell<sup>4</sup>

Received 31 August 2010; revised 23 December 2010; accepted 4 January 2011; published 16 March 2011.

[1] We present an original study of the dynamical changes measured in the far tail at  $X_{GSM} \approx -255 R_E$ , onboard STEREO-B, related to very weak substorm activity ( $AE < 100$  nT). Three weak auroral electrojet perturbations are well correlated with motions of the far tail in which the spacecraft passes from the lobe to the boundary layer or to the magnetosheath. These boundary motions can hardly be related to a plasmoid as a widening of the tail is expected from such a high-pressure structure. Furthermore, for one of the AE enhancements, ground measurement of auroral luminosity and ground magnetic field provided a precise timing of the substorm onset, thus allowing estimation of the propagation speed of the tail disturbance, supposing it is initiated at  $\sim 20 R_E$  in the midtail. The computed velocity, 1800 km/s, much greater than the typical plasmoid propagation speed, implies that the tail disturbance is due to a large-scale wave propagating inside the lobe, initiated inside the inner plasma sheet at substorm onset and linked to current disruption and/or magnetic reconnection.

**Citation:** Sauvaud, J.-A., A. Opitz, L. Palin, B. Lavraud, C. Jacquy, L. Kistler, H. U. Frey, J. Luhmann, D. Larson, and C. T. Russell (2011), Far tail ( $255 R_E$ ) fast response to very weak magnetic activity, *J. Geophys. Res.*, *116*, A03215, doi:10.1029/2010JA016077.

### 1. Introduction

[2] Assessing the large-scale dynamics of the magnetospheric system during substorms has motivated a number of studies in the recent years and is one of the main areas of magnetospheric research. Substorms are known to produce systematic and repeatable signatures in the magnetic field and plasma in various radial distances in the magnetotail.

[3] A repeatable signature in the midtail plasma sheet ( $\sim 20\text{--}30 R_E$ ) for substorms is tailward plasma flow with a southward magnetic field structure. *McPherron et al.* [1973] and *Russell and McPherron* [1973] applied the magnetic reconnection theory to magnetic substorm phenomena and proposed the “near-Earth neutral line” (NENL) model, which is one of the most successful candidates to explain the release and transport of stored energy in the magnetotail [*Hones*, 1979; *Baker et al.*, 1996]. It has been proposed that magnetic reconnection takes place in the expansion phase at radial distances of  $20\text{--}30 R_E$ . Plasmoids are created there and travel tailward at high speeds. They constitute a dominant substorm signature beyond  $100 R_E$  as shown by satellite measurements made from about  $100$  to  $210 R_E$  [*Nagai et al.*, 1994].

[4] The partial disruption of the cross-tail current is detected inside the lobe, near the time of substorm onset, as a decrease of the total magnetic field which continues during the substorm expansion phase. The magnetic field in the lobe recovers during the substorm recovery phase. While the measured magnetic field integrates the effect of all the disrupted parts of the tail current, a propagation effect can still be seen from dual-spacecraft lobe measurements [*Jacquy et al.*, 1993]. The disruption of the current itself propagates tailward in the midtail with velocities of the order of  $200\text{--}300$  km/s [*Jacquy et al.*, 1991; *Ohtani et al.*, 1992].

[5] Direct comparisons of IMP-8 midtail measurements of the cross tail current disruption and of distant effects induced by the passage of a plasmoid in the far tail onboard ISEE-3 have also been reported [*Sauvaud et al.*, 1996]. Observations of plasmoids are in fact highly correlated with substorm onsets in view of magnetic field data observed at ground stations and energetic particle data from geosynchronous satellites [*Moldwin and Hughes*, 1993; *Nagai et al.*, 1994]. In the tail lobe, a traveling compression region (TCR) is often observed and is interpreted to be a remote manifestation of a plasmoid passage [*Mezawa*, 1975; *Slavin et al.*, 1993; *Slavin et al.*, 2005].

[6] For one of the AE enhancement presented here, ground measurement of auroral luminosity has provided a precise timing of the substorm onset and has allowed to obtain an estimation of the propagation speed of the tail disturbance, supposing it begins at  $\sim 20 R_E$  in the midtail. The computed velocity between the midtail and the location of STEREO-B spacecraft in the far tail at  $X_{GSM} = -255 R_E$ , 1800 km/s, greatly exceeds the typical plasmoid propagation

<sup>1</sup>IRAP-University of Toulouse, CNRS, Toulouse, France.

<sup>2</sup>EOS, University of New Hampshire, Durham, New Hampshire, USA.

<sup>3</sup>Space Sciences Laboratory, University of California, Berkeley, California, USA.

<sup>4</sup>Institute of Geophysics and Planetary Physics, University of California, Los Angeles, California, USA.

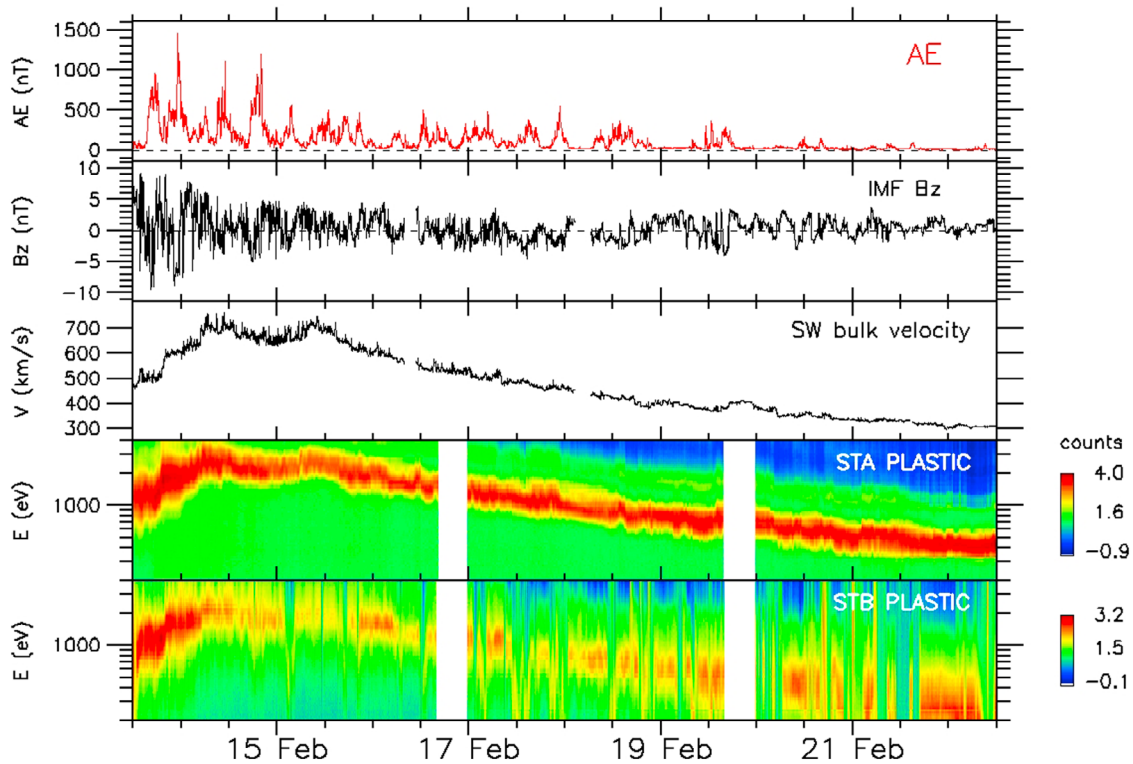


**Figure 1.** From top to bottom, the variation of the AE index, of the Bz component of the Interplanetary Magnetic Field (IMF) and of the solar wind velocity. These parameters have been extracted from the OMNI Combined, Definitive, 1 AU 1 min IMF and Plasma data. The fourth and fifth panels show the energy spectrograms of protons measured in solar wind onboard STEREO-A and similar measurements performed onboard STEREO-B on its travel away from the Moon. In order to compare ion data from STEREO-A (directed flux) and STEREO-B (directed to nearly isotropic flux), counts summed over all deflection angles are used. These measurements are performed once per minute during 409 ms.

velocity. This large propagation speed implies that the tail disturbance is due to a large-scale Alfvén wave propagating inside the lobe which tends to reduce the magnetic pressure. Its effect can be measured because on 21 February 2007, STEREO-B is very close to the tail boundary of the far tail. This first measurement of the effect of such a large-scale wave sheds light on the response of the far tail to substorms and will have important implications on the tail dynamics modeling during magnetospheric disturbances.

## 2. Observations

[7] When the two STEREO spacecraft were launched on 25 October 2006, they were first placed in a highly eccentric orbit around Earth [Kaiser *et al.*, 2008]. For the first few weeks, the two spacecraft stayed fairly close to each other as they lined up for their close encounter with the Moon one month into the mission. As they flew by, the Moon’s gravity flung the two spacecraft away from Earth. The “Ahead” spacecraft is flung completely away from Earth, and becomes a satellite of the Sun, while the “Behind” spacecraft curves back to fly past the Moon a second time six weeks later, on 21 January 2007, and was flung in the opposite direction. The orbits of the two STEREO spacecraft are both more eccentric than Earth’s, with the “Ahead” spacecraft orbiting slightly inside Earth’s orbit, and the “Behind” spacecraft

orbiting slightly outside. Because of these slight differences in the average distance from the Sun, the two spacecraft slowly drift away from Earth in opposite directions. After the last Moon flyby of STEREO-B, the spacecraft was skimming along the tail of the magnetosphere at distances ranging from 200 to 350  $R_E$  allowing the dynamics of the distant tail to be studied.

[8] Figure 1 provides an overview of the auroral activity, and of the solar wind variations for the period between 13 February and 22 February 2007 together with plasma measurements performed onboard the two STEREO spacecraft. From top to bottom, Figure 1 displays the variation of the AE index, of the Bz component of the Interplanetary Magnetic Field (IMF) and of the solar wind velocity. These two last parameters have been extracted from the OMNI Combined, Definitive, 1 AU 1 min IMF and Plasma data (<http://omniweb.gsfc.nasa.gov>). The two last panels show the energy spectrograms of protons measured in the solar wind onboard STEREO-A and similar measurements performed onboard STEREO-B on its travel away from the Moon [Galvin *et al.*, 2008]. Figure 1 clearly shows the decreasing speed of the solar wind after the encounter of a fast stream. The magnetic activity on Earth also generally decreases from the beginning to the end of the period and the largest activity periods correspond to high solar wind velocities

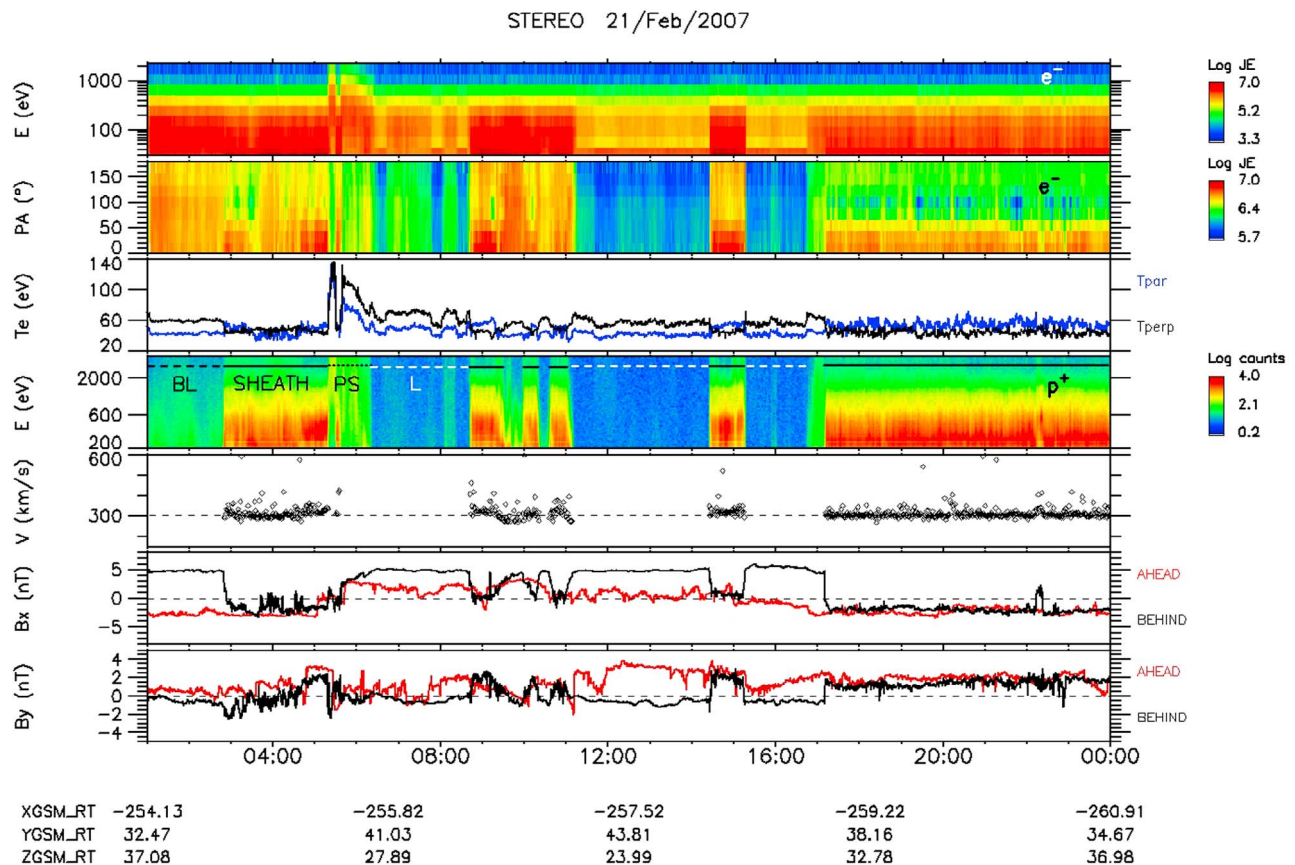


**Figure 2.** The first to fifth panels are from STEREO-B. The first panel gives the SWEA electrons energy spectrogram between 45 and 2400 eV, the second panel presents the electron pitch angle distribution at 150 eV, and the third panel provides the parallel and perpendicular temperatures of the electrons. The fourth panel gives the proton energy spectrogram for energies between 0.2 and 4 keV. The identification of the various regions encountered by STEREO-A are given by coded horizontal lines associated with boundary layer (BL), magnetosheath (SHEATH), plasma sheet (PS) and lobe (L). For each electron spectrogram, the colors are coding energy fluxes expressed in  $\text{keV}/(\text{cm}^2 \text{ s sr keV})$ . For the proton spectrogram, colors are coding counts ( $\propto \text{JE}$ ). The fifth panel provides the proton speed when it can be computed with a good accuracy from the solar wind entrance of the PLASTIC analyzer. The sixth and seventh panels display the Bx and By components of the magnetic field measured onboard STEREO-B (black) and STEREO-A (red). The STEREO-A data have been shifted to account for the delay deduced from the solar wind velocity and from the distance between the two spacecraft.

and negative (southward), fluctuating, Bz, as expected [e.g., Russell and McPherron, 1973, 1974; Akasofu, 1981].

[9] The comparison of STEREO-A and -B measurements clearly indicates that while the two spacecraft grossly measure the same time profiles of the ion energy, STEREO-B observed times when there is a disappearance of the solar wind plasma. This spacecraft went many times from the magnetosheath, where the plasma is hotter than in the solar wind, into the lobe region of the distant tail, filled with tenuous plasma. In fact the encounter of the distant magnetosheath-boundary layer/lobe interface begins on 14 February around 1500 UT while STEREO B was at  $213 R_E$  away from the Earth and lasts until 2 March 2007 when spacecraft B definitively exits into the solar wind at  $350 R_E$  from Earth.

[10] We will focus on the tail dynamics recorded on 21 February 2007 between 0100 and 2400 UT, which coincides with a weak magnetic activity period, the Auroral Electrojet, AE, index being smaller than 100 nT (Figure 1).

Figure 2 presents the STEREO data recorded on that day, the spacecraft being located at  $X_{\text{GSM}} = -255 R_E$ . The upper panel gives the STEREO-B electron energy spectrogram between 45 and 2400 eV. The second from the top presents the STEREO-B electron pitch angle distribution at 150 eV. These electron measurements were obtained by the Solar Wind Electron Analyzer (SWEA) [Sauvaud et al., 2008] which is included in the IMPACT suite of instruments for in situ measurements [Luhmann et al., 2008]. The third panel provides the parallel and perpendicular temperatures of the electrons for  $E > 45$  eV. The fourth panel from the top gives the STEREO-B proton energy spectrogram at energies between 0.2 and 4 keV [see Galvin et al., 2008]. The fifth panel provides the velocity of protons when it can be computed with a good accuracy from the solar wind entrance of the PLASTIC analyzer. The two bottom panels display the GSM Bx and By components of the magnetic field measured onboard STEREO-B (black) and STEREO-A (red)

[Acuña *et al.*, 2008]. The STEREO-A data have been shifted to account for the delay deduced from the solar wind velocity and from the distance between the two spacecraft. The spacecraft are separated by  $\sim 740 R_E$  ( $4.7 \times 10^6$  km) along the Sun-Earth direction; STEREO-A being located at  $\{X_{GSM} = 481 R_E, Y_{GSM} = -301 R_E, Z_{GSM} = -153 R_E\}$  and STEREO-B at  $\{X_{GSM} = -255 R_E, Y_{GSM} = 39 R_E, Z_{GSM} = 30 R_E\}$ . Note that STEREO-B is at positive and relatively small  $Y_{GSM}$  and  $Z_{GSM}$  values, with  $Y_{GSM} > Z_{GSM}$ , (both lower than  $44 R_E$  throughout 21 February 2007), that is ‘close’ to the expected position of the far-tail dusk magnetopause, extrapolated from its position closer to the Earth. On the side of the tail different regions: magnetosheath, boundary layer, plasma sheet and lobe, are expected to be close to each other [Christon *et al.*, 1998; Eastman *et al.*, 1998]. The comparison of the Bx components of the magnetic field onboard the two spacecraft indicates clearly two main regimes alternatively encountered: periods when the two Bx components are very similar, despite the spacecraft separation, e.g., between 0300 and 0500 UT or between 1710 and 2400 UT. During these periods, STEREO-A is inside the solar wind, while STEREO-B is inside the far tail magnetosheath as shown also by high electron fluxes at energies lower than 500 eV, with parallel and perpendicular electron temperatures of the order of 40–50 eV, higher than those of the solar wind. Similarly, the proton energy spectrogram and the deduced flow velocity around 300 km/s, slightly lower than the solar wind velocity displayed in Figure 1, confirm that the spacecraft is inside the distant magnetosheath. Inside these regions, the electron fluxes are mostly collimated along the magnetic field.

[11] On the contrary, there are periods when the Bx component of the magnetic field measured on STEREO-B is very different from that of STEREO-A., e.g., between 0100 and 0300 UT, 0540 and 0840 UT, 1100 and 1400 UT, and finally between 1510 and 1710 UT. During these periods, reduced fluxes of electrons are measured, and they have nearly isotropic pitch angle distributions. Moreover, the proton fluxes there are much lower than inside the magnetosheath at low energies. In the fourth panel of Figure 2, we indicate the proposed identification of the various regions encountered by STEREO-B by coded horizontal lines associated with for boundary layer (BL), magnetosheath (Sheath), plasma sheet (PS), and lobe (L). Between 0100 UT and 0300 UT, the magnetic field is enhanced, like inside the lobes but electron energy spectra are still “magnetosheath-like.” We identify this region as the boundary layer. The other periods with enhanced Bx and very weak electron fluxes (0540 to 0840 UT and 1100 to 1420 UT) are identified as the lobe. A different region is briefly encountered between 0530 and 0610 UT characterized by electrons at energies higher than 700 keV and protons up to 4 keV. The electron temperature can exceed 100 eV. This region, identified as the distant plasma sheet, is also characterized by energetic oxygen [Kistler *et al.*, 2010]. To summarize, the satellite passes from the magnetosheath to the boundary layer/lobe of the distant tail many times during that day and makes a brief encounter with the plasma sheet.

[12] These crossings of the tail boundary by STEREO-B are very frequent during an extended period starting from 14 February 2007 as the tail is moving around a lot. The

multiple crossings of the magnetopause presented in Figure 2 occur during a period when the magnetic activity is extremely low (Figure 1). This is clearly exemplified in Figure 3 which displays from 0100 to 1900 UT the variations of the AE index, the Bx component of the magnetic field recorded at  $X_{GSM} \sim 255 R_E$  onboard STEREO-B and the electron density measured by the Solar Wind Electron Analyzer (SWEA). The three vertical dashed lines indicate the onset of AE enhancements. It must be stressed that the overall values of the AE index are very small, lower than 100 nT. Despite this low activity, there is a striking general correlation between the auroral activity and the dynamics of the far tail. The three main AE enhancement episodes are related to the exit of STEREO-B into the magnetosheath while during quiet intervals, the satellite returns into the lobe of the distant tail. However, after 1700 UT, the satellite again exits into the magnetosheath while the magnetic activity stays very low, which could be an indication that the spacecraft is very close to the magnetopause during the whole period.

[13] The weak AE enhancements can tentatively be associated with weak substorms. An examination of the nightside auroral magnetograms indeed shows weak and localized magnetic bays. However, no plasma injection is recorded at geostationary orbit, which is quite common for such low auroral disturbances. For the AE enhancement beginning around 0830 UT, direct evidence for the occurrence of a substorm is provided by THEMIS/GBO all-sky camera data in “white light” and magnetic field variations recorded at the INUVIK station located in the northwest part of Canada at a corrected magnetic latitude of  $71.2^\circ$ . A keogram illustrating the variation of the auroral luminosity in the form of a latitude-time spectrogram is given in Figure 4, while the H components and Z components of the INUVIK magnetic field are given in Figure 5. A narrow band of auroral luminosity is drifting equatorward from 0800 to 0828 UT. The rotation of the station under the oval within 28 min cannot explain the magnitude of the equatorward motion of the oval seen there. This is the equatorward motion of the aurora and expansion of the polar cap during substorm growth phase which is at the root of the observation. Then at  $\sim 0828$  UT ( $\sim 22$ h MLT) the aurora breaks up and auroral forms quickly propagate northward with visible intensifications at 0828 UT, 0833 UT and 0841 UT. This represent a clear onset of a substorm associated with the minor AE enhancement seen at 0828 UT in Figure 3. Concurrently, the H component of the magnetic field at Inuvik shows a clear negative bay while the Z component first negative and then positive indicates that the westward localized electrojet quickly passed from the north to the south of the station. This event where the activity began in the preexisting aurora and expands poleward looks like a normal substorm onset. The substorm occurs along a contracted auroral oval, typical of low magnetic activity periods. The cross-tail current is quite weak during such episode so that, in the midnight sector, the apex of a field line is, for a fixed latitude, located closer to the Earth than for more enhanced tail current [e.g., Tsyganenko, 1995]. This leads the boundary between diffuse and discrete aurora to move northward with respect to their position during more disturbed times. For the 21 February 2007 case discussed there, we checked, using the DMSP F16 particle data

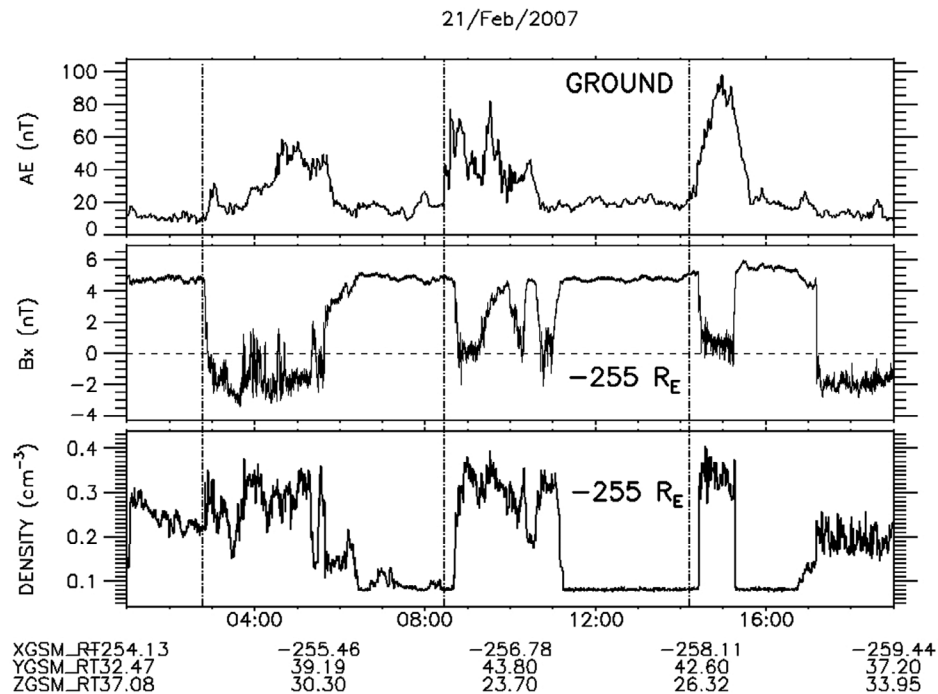


**Figure 3.** From 0100 to 1900 UT on 21 February 2007: the variations of the AE index, the Bx component of the magnetic field recorded at  $X_{\text{GSM}} = -255 R_E$  onboard STEREO-B, and the electron density measured by the Solar Wind Electron Analyzer (SWEA) on STEREO-B. The three vertical dashed lines indicate the onset of AE enhancements.

available (Southern Hemisphere), the latitude of the boundary between diffuse and discrete auroras, i.e., where substorms are expected to be initiated: it was located, at high magnetic latitudes:  $-68.8^\circ$  at MLT = 0016 and  $-70.5^\circ$  at MLT = 0147.

[14] This substorm onset precedes the exit of the STEREO-B satellite into the magnetosheath at 0841:50 UT by less than 14 min. If we assume that the two events are related (Figure 3), we find a propagation velocity of about 1800 km/s for the information to travel from about  $-20 R_E$ , where the substorm is expected to be initiated, to the STEREO-B location at  $X = -255 R_E$ . The  $20 R_E$  value for the substorm onset location take into account the results of different studies of similar events corresponding to AE values  $\leq 100$  nT by *Sauvaud et al.* [1999], *Nishida et al.* [1997], *Angelopoulos et al.* [2008], and *Kubyshkina et al.* [2009]. Using various methods, including dedicated magnetic field models, correlations between optical data and in situ spacecraft measurements in the tail (Geotail, Interball, THEMIS), these authors reached the conclusion that these weak substorms occurring during quiet periods were activated at distances ranging between 8 and  $20 R_E$  from the Earth.

### 3. Discussion

[15] It is well known that substorms produce systematic and repeatable signatures in magnetic field and plasmas at various radial distances in the magnetotail. A scenario for plasmoid formation in the Earth's magnetotail was proposed by *Russell* [1974] and *Hones* [1979] on the basis of satellite observations. A large-scale magnetic island containing a hot

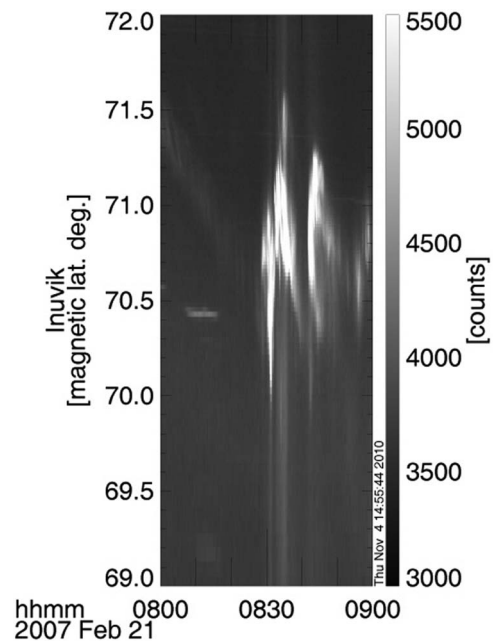


**Figure 4.** Keogram giving the latitudinal variation of the auroral luminosity recorded at INUVIK. These “white light” data are from THEMIS ground based observatories. A narrow band of auroral luminosity is drifting equatorward from 0800 to 0828 UT on 21 February 2007 during the growth phase of the substorm. At  $\sim 0828$  UT the aurora breaks up.

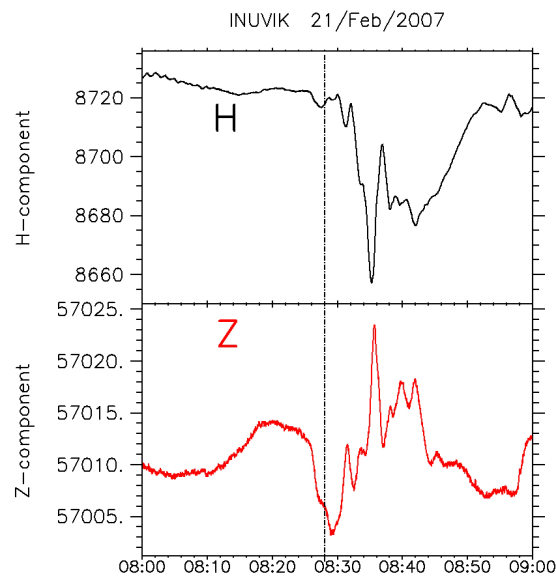


**Figure 5.** H and Z component of the ground magnetic field at INUVIK. The vertical dot-dashed line marks the time of the auroral luminosity intensification (see Figure 4).

and dense plasma is formed, probably in association with magnetic reconnection which is initiated at the near-Earth neutral line, and the magnetic island, or so-called plasmoid, is propagating tailward. Observations of plasmoids are highly correlated with substorm onsets [Moldwin and Hughes, 1991, 1992, 1993, 1994; Nagai *et al.*, 1994]. Plasmoids originate at about  $20\text{--}30 R_E$  downtail and have been observed up to about  $200 R_E$ ; typical tailward speeds are several hundreds of km/s. A statistical study performed by Ieda *et al.* [1998], on the basis of Geotail data, shows that

the plasmoids are accelerated in the downtail direction from  $400 \pm 200$  km/s to  $700 \pm 300$  km/s from the near to the middle tail; then, it is suggested that they decelerate to  $600 \pm 200$  km/s as they travel to the distant tail. Taking the upper limits of these propagation velocities, i.e., 600 km/s between  $20 R_E$  and  $40 R_E$ , 1000 km/s between  $40$  and  $150 R_E$  and finally 800 km/s between  $150$  and  $255 R_E$ , would imply a time delay of 29 min between the substorm onset at 0828 UT and the response of the distant tail at the STEREO-B location, instead of the observed 14 min. (Hones *et al.* [1984] found a propagation time of 30 min to reach ISEE-3 at  $220 R_E$ .) Note that this response is a magnetopause motion leading the STEREO-B spacecraft to exit into the magnetosheath.

[16] Magnetopause motions in the far tail have already been shown to be induced by substorm associated processes: a study performed from simultaneous IMP-8 and ISEE-3 data by Sauvaud *et al.* [1996] has shown a characteristic time delay of 40 min between cross-tail current disruption onset occurring in the near-Earth plasma sheet and the enhancement of the tail diameter at  $205 R_E$ . The observed signatures were in agreement with the concept of the ejection of plasmoids from the magnetospheric tail and the tailward propagation of a compression region with enhanced pressure, so that the ISEE-3 satellite initially in the distant magnetosheath was entering the magnetosphere when the high-pressure region reached its location.

[17] In the study presented here, the opposite motion of the magnetopause is detected: the observations are in agreement with a shrinking of the far tail, quickly (14 min) following a substorm onset. It is thus difficult to reconcile this observation with the propagation of a large-scale plasmoid which would induce a widening of the tail as already observed onboard ISEE-3. However, it is not possible to firmly rule out that  $\sim 15$  min or more after STEREO-B is led

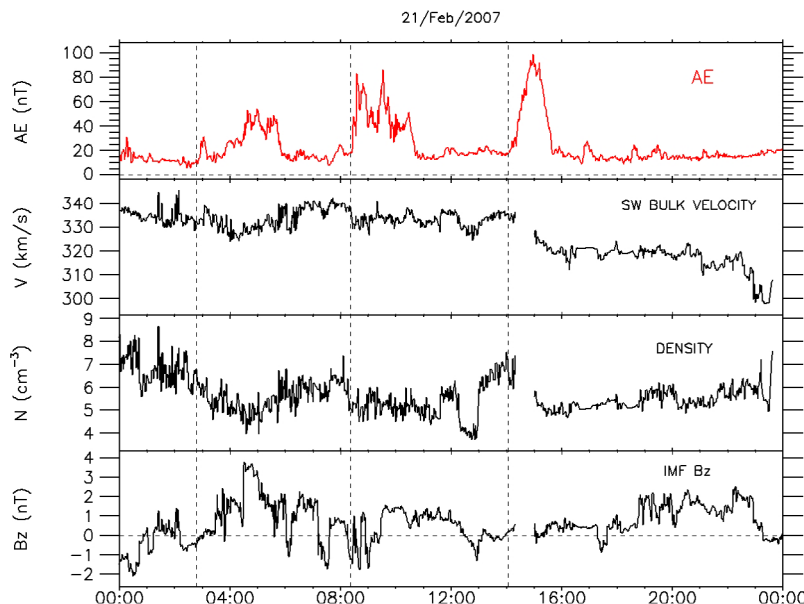


**Figure 6.** From top to bottom, the AE index, the velocity and the density of the solar wind, and the Bz component of the IMF at 1 AU on 21 February 2007 (these data have been extracted from the OMNI Combined, Definitive, 1AU 1 min IMF and Plasma data).

to pass into the magnetosheath, a plasmoid launched from the midtail is traveling in the far tail, undetected by the satellite.

[18] A possibility to explain the short delay and the apparent shrinking/flapping of the tail is that its deformation is related to a large-scale wave propagating along the tail. In fact, the Earth magnetotail has long been known to support the propagation of low-frequency waves. Its stretched magnetic field structure behaves indeed as an efficient MHD waveguide [Allan and Wright, 2000]. The initial perturbation of the plasma sheet can be excited in the midtail by a sudden force field which may correspond to a pressure burst or a current disruption. As recently shown by Fruit and Louarn [2011], with a finite  $B_z$  component of the tail magnetic field, the linear response of the plasma sheet is composed of two wave trains: a first wavefront identified as a sound wave propagates isotropically at the sonic speed from the initial burst and an eigenmode structure develops next, but it propagates at a much lower speed along the  $x$  axis and contains relatively little energy. About 99% of the initial energy of the burst is carried away by the sound wave. We expect that the pressure wave quickly reaches the lobe–plasma sheet interface and the lobes react as a waveguide with a low density and an almost zero  $B_z$  component. In that case, the perturbation launches an Alfvén wave propagating at high velocities, as estimations of the Alfvén velocity,  $B/(\mu_0\rho)^{1/2}$ , in the magnetotail lobe give values between 1000 and >3000 km/s, depending on the distance to the Earth [e.g., Mazur and Leonovich, 2006].

[19] Finally, we also have to check if the measured tail disturbances could directly originate in the solar wind. Figure 6 displays the AE index, the solar wind velocity and density, and the GSM  $B_z$  component of the magnetic field. These solar wind data have been extracted from the OMNI Combined, Definitive, 1 AU 1 min IMF and Plasma data. There is no evidence for pressure enhancement. On the contrary, the AE enhancements correspond to slight decreases in density and velocity which should be associated with an inflation of the tail. Note also that the  $B_z$  is generally positive with small negative excursions, particularly before the first two AE enhancements, and there is no obvious correlations between any small changes in the  $B_z$  components and the observed magnetopause crossings. Note furthermore that looking at the total B field onboard STEREO-B, which is almost equal to its  $B_x$  component, no clear effect of compression of the tail is locally seen.

#### 4. Conclusion

[20] The large-scale dynamic evolution of the magnetotail in relation to substorms is most commonly understood and described in terms of magnetic reconnection, neutral line formation, and plasmoid ejection into the distant tail, as well as current disruption and diversion in the inner tail. We have presented a case study of the dynamical changes seen in the far tail ( $\sim 255 R_E$ ) related to enhanced but weak to very weak geomagnetic activity (AE < 100 nT). STEREO-B was located close to the boundary separating the lobe from the boundary layer/magnetosheath. During a 24 h period, three very weak auroral electrojet perturbations are surprisingly well correlated with motions of the far tail. The spacecraft passes from the lobe to the boundary layer or to the mag-

netosheath, very shortly after each AE perturbation. These boundary motions can hardly be related to a plasmoid as a widening of the tail is expected from such a high-pressure structure. Previous work has indeed shown, as expected, that plasmoids lead a satellite located in the distant magnetosheath to pass inside the lobe [e.g., Sauvaud et al., 1996], i.e., the reverse motion of what is observed for the cases presented here.

[21] For one of the AE enhancement, ground measurement of auroral luminosity has provided a precise timing of the substorm onset related to the AE enhancement, so that an estimation of the propagation speed of the tail disturbance, supposing it begins at  $\sim 20 R_E$  in the midtail, can be computed. This speed, 1800 km/s, greatly exceeds the typical plasmoid propagation velocity (760 km/s) computed from a large set of events recorded by the Geotail spacecraft [Jeda et al., 1998]. This fast propagation speed implies that the tail disturbance is due to a large-scale wave propagating inside the lobe, which tends to reduce the magnetic pressure. Its effect can be measured because STEREO-B is located during this period of 21 February 2007, very close to the tail boundary. To our knowledge, this is the first measurement reporting such a fast coupling between the mid and far tail during substorms. This effect may have been “embedded” in complex changes for larger activity. This sheds light on the response of the far tail to substorms and will have implications on the tail dynamics modeling during magnetospheric disturbances.

[22] **Acknowledgments.** Data used in this paper were acquired by satellites operated by NASA. We acknowledge NASA contract NASS-02099 and V. Angelopoulos for use of data from the THEMIS Project. Specifically, we thank S. Mende and E. Donovan for use of the ASI data, and the CSA for logistical support in fielding and data retrieval from the GBO stations. The SWEA sensor heads on the two STEREO spacecraft were funded by the French CNES and CNRS. The DMSP particle detectors used to locate the boundary between diffuse and discrete auroras were designed by Dave Hardy of AFRL, and data were obtained from JHU/APL. Solar wind data at 1 AU have been obtained from CDAWEB and AE data from WDC-2. We thank E. Penou (CNRS) for providing the software for data displays.

[23] Masaki Fujimoto thanks the reviewers for their assistance in evaluating this paper.

#### References

- Acuña, M. H., D. Curtis, J. L. Scheifele, C. T. Russell, P. Schroeder, A. Szabo, and J. G. Luhmann (2008), The STEREO/IMPACT magnetic field experiment, *Space Sci. Rev.*, *136*, 203–226, doi:10.1007/s11214-007-9259-2.
- Akasofu, S. I. (1981), Energy coupling between the solar wind and the magnetosphere, *Planet. Space Sci.*, *28*, 121–190.
- Allan, W., and A. N. Wright (2000), Magnetotail waveguide: Fast and Alfvén waves in the plasma sheet boundary layer and lobe, *J. Geophys. Res.*, *105*, 317–328, doi:10.1029/1999JA900425.
- Angelopoulos, V., et al. (2008), Tail reconnection triggering substorm onset, *Science*, *321*, 931–935, doi:10.1126/science.1160495.
- Baker, D. N., T. I. Pulkkinen, V. Angelopoulos, W. Baumjohann, and R. L. McPherron (1996), Neutral line model of substorms: Past results and present view, *J. Geophys. Res.*, *101*, 12,975–13,010, doi:10.1029/95JA03753.
- Christon, S. P., et al. (1998), Magnetospheric plasma regimes identified using Geotail measurements 2. Statistics, spatial distribution, and geomagnetic dependence, *J. Geophys. Res.*, *103*, 23,521–23,542, doi:10.1029/98JA01914.
- Eastman, T. E., et al. (1998), Magnetospheric plasma regimes identified using Geotail measurements 1. Regime identification and distant tail variability, *J. Geophys. Res.*, *103*, 23,503–23,520, doi:10.1029/98JA01915.

- Fruit, G., and P. Louarn (2011), On the propagation of MHD eigenmodes in a 2-D magnetotail, *Ann. Geophys.*, *29*, 19–30, doi:10.5194/angeo-29-19-2011.
- Galvin, A. B., et al. (2008), The Plasma and Suprathermal Ion Composition (PLASTIC) investigation on the STEREO observatories, *Space Sci. Rev.*, *136*, 437–486, doi:10.1007/s11214-007-9296-x.
- Hones, E. W., Jr. (1979), Transient phenomena in the magnetotail and their relation to substorms, *Space Sci. Rev.*, *23*, 393–410, doi:10.1007/BF00172247.
- Hones, E. W., Jr., D. N. Baker, S. J. Bame, W. C. Feldman, J. T. Gosling, D. J. McComas, R. D. Zwickl, J. A. Slavin, E. J. Smith, and B. T. Tsurutani (1984), Structure of the magnetotail at 220 RE and its response to geomagnetic activity, *Geophys. Res. Lett.*, *11*, 5–7, doi:10.1029/GL011i001p00005.
- Ieda, A., S. Machida, T. Mukai, Y. Saito, T. Yamamoto, A. Nishida, T. Terasawa, and S. Kokubun (1998), Statistical analysis of the plasmoid evolution with Geotail observations, *J. Geophys. Res.*, *103*, 4453–4465, doi:10.1029/97JA03240.
- Jacquey, C., J. A. Sauvaud, and J. Dandouras (1991), Location and propagation of the magnetotail current disruption during substorm expansion: Analysis and simulation of an ISEE multi-onset event, *Geophys. Res. Lett.*, *18*, 389–392, doi:10.1029/90GL02789.
- Jacquey, C., J. A. Sauvaud, J. Dandouras, and A. Korth (1993), Tailward propagating cross-tail current disruption and dynamics of near-Earth tail: A multi-point measurement analysis, *Geophys. Res. Lett.*, *20*, 983–986, doi:10.1029/93GL00072.
- Kaiser, M. L., T. A. Kucera, J. M. Davila, O. C. St. Cyr, M. Guhathakurta, and E. Christian (2008), The STEREO Mission: An introduction, *Space Sci. Rev.*, *136*, 5–16, doi:10.1007/s11214-007-9277-0.
- Kistler, L. M., et al. (2010), Escape of O<sup>+</sup> through the distant tail plasma sheet, *Geophys. Res. Lett.*, *37*, L21101, doi:10.1029/2010GL045075.
- Kubyskhina, M., V. Sergeev, N. Tsyganenko, V. Angelopoulos, A. Runov, H. Singer, K. H. Glassmeier, H. U. Auster, and W. Baumjohann (2009), Toward adapted time-dependent magnetospheric models: A simple approach based on tuning the standard model, *J. Geophys. Res.*, *114*, A00C21, doi:10.1029/2008JA013547.
- Luhmann, J. G., et al. (2008), STEREO IMPACT investigation goals, measurements, and data products overview, *Space Sci. Rev.*, *136*, 117–184, doi:10.1007/s11214-007-9170-x.
- Mazur, V. A., and A. S. Leonovich (2006), ULF hydromagnetic oscillations with the discrete spectrum as eigenmodes of MHD-resonator in the near-Earth part of the plasma sheet, *Ann. Geophys.*, *24*, 1639–1648, doi:10.5194/angeo-24-1639-2006.
- McPherron, R. L., C. T. Russell, and M. P. Aubry (1973), Satellite studies of magnetospheric substorms on August 15, 1968, 9. Phenomenological model for substorms, *J. Geophys. Res.*, *78*, 3131–3149, doi:10.1029/JA078i016p03131.
- Maezawa, K. (1975), Magnetotail boundary motion associated with geomagnetic substorms, *J. Geophys. Res.*, *80*, 3543–3548, doi:10.1029/JA080i025p03543.
- Moldwin, M. B., and W. J. Hughes (1991), Plasmoids as magnetic flux ropes, *J. Geophys. Res.*, *96*, 14,051–14,064, doi:10.1029/91JA01167.
- Moldwin, M. B., and W. J. Hughes (1992), Multi-satellite observations of plasmoids: IMP-8 and ISEE-3, *Geophys. Res. Lett.*, *19*, 1081–1096, doi:10.1029/92GL00779.
- Moldwin, M. B., and W. J. Hughes (1993), Geomagnetic substorm association of plasmoids, *J. Geophys. Res.*, *98*, 81–88, doi:10.1029/92JA02153.
- Moldwin, M. B., and W. J. Hughes (1994), Observation of earthward and tailward propagating flux rope plasmoids: Expanding the plasmoid model of geomagnetic substorms, *J. Geophys. Res.*, *99*, 183–198, doi:10.1029/93JA02102.
- Nagai, T., K. Takahashi, H. Kawano, T. Yamamoto, S. Kokubun, and A. Nishida (1994), Initial GEOTAIL survey of magnetic substorm signatures in the magnetotail, *Geophys. Res. Lett.*, *21*, 2991–2994, doi:10.1029/94GL01420.
- Nishida, A., T. Mukai, T. Yamamoto, Y. Saito, S. Kokubun, and R. P. Lepping (1997), Traversal of the nightside magnetosphere at 10 to 15 Re during northward IMF, *Geophys. Res. Lett.*, *24*, 939–942, doi:10.1029/97GL00219.
- Ohtani, S., S. Kokubun, and C. T. Russell (1992), Radial expansion of the tail current disruption during substorms: A new approach to the substorm onset region, *J. Geophys. Res.*, *97*, 3129–3136, doi:10.1029/91JA02470.
- Russell, C. T. (1974), The solar wind and magnetospheric dynamics, in *Correlated Interplanetary and Magnetospheric Observations*, edited by D. E. Page, pp. 3–47, D. Reidel, Dordrecht, Netherlands.
- Russell, C. T., and R. L. McPherron (1973), The magnetotail and substorms, *Space Sci. Rev.*, *11*, 111–122.
- Sauvaud, J.-A., C. Jacquey, T. Beutier, C. Owen, R. P. Lepping, C. T. Russell, and R. J. Belian (1996), Large-scale dynamics of the magnetospheric tail induced by substorms: A multisatellite study, *J. Geomag. Geoelectr.*, *48*, 675–686.
- Sauvaud, J.-A., D. Popescu, D. Delcourt, G. Parks, M. Brittacher, V. Sergeev, R. Kovrazhkin, T. Mukai, and S. Kokubun (1999), Sporadic plasma sheet ion injections into the high-altitude auroral bulge: Satellite observations, *J. Geophys. Res.*, *104*, 28,565–28,586, doi:10.1029/1999JA900293.
- Sauvaud, J.-A., et al. (2007), The IMPACT Solar Wind Electron Analyzer (SWEA), *Space Sci. Rev.*, *136*, 227–239, doi:10.1007/s11214-007-9174-6.
- Shirai, H., T. K. Takada, and T. Mukai (2005), Velocity of magnetic neutral lines in the magnetotail, *Adv. Space Res.*, *36*, 1878–1882, doi:10.1016/j.asr.2003.09.074.
- Slavin, J. A., M. F. Smith, E. L. Mazur, D. N. Baker, E. W. Hones Jr., T. Iyemori, and E. W. Greenstadt (1993), ISEE 3 observations of traveling compression regions in the earth's magnetotail, *J. Geophys. Res.*, *98*, 15,425–15,446, doi:10.1029/93JA01467.
- Slavin, J. A., E. I. Tanskanen, M. Hesse, C. J. Owen, M. W. Dunlop, S. Imber, E. A. Lucek, A. Balogh, and K.-H. Glassmeier (2005), Cluster observations of traveling compression regions in the near-tail, *J. Geophys. Res.*, *110*, A06207, doi:10.1029/2004JA010878.
- Tsyganenko, N. A. (1995), Modeling the Earth's magnetospheric magnetic field confined within a realistic magnetopause, *J. Geophys. Res.*, *100*, 5599–5612, doi:10.1029/94JA03193.

H. U. Frey, D. Larson, and J. Luhmann, Space Sciences Laboratory, University of California, 7 Gauss Way, Berkeley, CA 94720, USA.

C. Jacquey, B. Lavraud, A. Opitz, L. Palin, and J.-A. Sauvaud, IRAP-University of Toulouse, CNRS, 9 av. du Colonel roche, BP 4346, F-31028 Toulouse, France. (jean-andre.sauvaud@cesr.fr)

L. Kistler, EOS, University of New Hampshire, Morse Hall, Durham, NH 03824, USA.

C. T. Russell, Institute of Geophysics and Planetary Physics, University of California, 603 Charles Young Dr. East, 3845 Slichter Hall, Los Angeles, CA 90095-1567, USA.